

# Rate-Limiting Mechanism in Iron Ore Sintering Process with Waste Gas Recycling

Veera Brahmacharyulu Angalakuditi<sup>1</sup>  · Sudhakar Karre<sup>1</sup> · Lokendra Raj Singh<sup>1</sup> · Saroj Sundar Baral<sup>2</sup>

Received: 7 August 2020 / Accepted: 13 December 2020 / Published online: 4 February 2021  
© The Indian Institute of Metals - IIM 2021

**Abstract** Recycling waste gas through the sinter bed has an advantage of saving solid fuel. Depending upon the amount of waste gas recycled and its CO content, an equivalent quantity of solid fuel is saved. FeO is one of the key indicators of fuel needed for sintering; its optimization is critical to the consistency in sinter quality. Sinter pot tests were conducted to identify the effect of varying amounts of waste gas recycled. FeO and Tumbler Index increased with increasing waste gas up to 30%. Beyond 40% waste gas recycled, Tumbler Index decreased and the disintegration of the sinter was noticed. Incidental variation in the rate of solid fuel in an industrial scale Sinter Plant with waste gas recycling arrangement has resulted in a large variation in FeO than expected. Above 20%, productivity got adversely affected and Tumbler Index dropped as oxygen in the recycled gas started dropping below 19%. The rate-limiting mechanism has been identified as the underlying reason for low FeO. The deficiency of oxygen has affected the combustion efficiency of solid fuel, and hence, fresh airflow has been optimized to maintain the productivity and quality parameters. The variation in the carbon rate was restricted to  $0.77 \pm 0.5$  kg/t, and oxygen was maintained above 19% to achieve consistent performance.

**Keywords** Iron ore sinter · Waste gas recycling · Wüstite · Rate-limiting step

## Abbreviations

<i>a</i>	Activity
BTP	Burn through point
BTT	Burn through temperature
CO	Carbon monoxide
dCr	Difference in carbon rate
dFeO	Difference in FeO
$\Delta G$	Free energy change
$\Delta H$	Enthalpy change
$\Delta S$	Entropy change
ESP	Electrostatic precipitator
FA Fan	Fresh air fan
FC	Fixed carbon
FeO	Wüstite
Fe <sub>2</sub> O <sub>3</sub>	Hematite
Fe <sub>3</sub> O <sub>4</sub>	Magnetite
LOI	Loss on ignition
NTP	Normal temperature and pressure
<i>p</i>	Partial pressure
ppm	Parts per million
RDI	Reduction degradation index
SFCA	Silico ferrite of calcium and aluminum
SWGR	Selective waste gas recycling
<i>t</i>	Temperature in Celsius
<i>T</i>	Temperature in Kelvin
TI	Tumbler Index
VM	Volatile matter
WGR	Waste gas recycling
WGR Fan	Waste gas recycling fan

✉ Veera Brahmacharyulu Angalakuditi  
angalakuditi.brahmacharyulu@jsw.in

<sup>1</sup> JSW Steel Ltd, Vijayanagar Works, Toranagallu, Karnataka 583275, India

<sup>2</sup> Department of Chemical Engineering, BITS Pilani KK Birla Goa Campus, Zuarinagar, Goa 403726, India

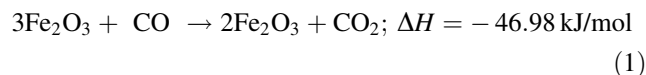
## 1 Introduction

Iron ore sintering is an agglomeration process, whose product, commonly known as *sinter*, is the major feed to Blast Furnace to produce hot metal. The hot metal is further refined in a converter to produce steel. In the iron ore sintering process, sinter mix consisting of the *finer* of iron ore, limestone, dolomite and solid fuel is mixed with water, granulated and charged on a traveling grate. The top layer is ignited, and the atmospheric air is continuously drawn through the bed. The heat released by the combustion of solid fuel helps in fusing the flux and hence slag formation. As the sintering process proceeds, the combustion zone travels down and the temperature of the waste gas below the Sinter Machine gradually rises. The solid fuel present in the sinter mix gets completely burnt at burn through point (BTP). The temperature of the waste gas at BTP is known as burn through temperature (BTT). Normally, BTT is in the range of 350–450 °C. The cooling of the sinter starts after BTP. As the slag gets solidified, the iron ore particles are bound together [1]. At the end of the Sinter Machine, the solidified sinter is discharged.

The physical and chemical properties of the sinter are critical to the performance of the Blast Furnace. The cold strength of the sinter is measured as TI and hot strength as RDI. The Fe<sub>2</sub>O<sub>3</sub> in the iron ore is reduced to Fe<sub>3</sub>O<sub>4</sub> and then to FeO, with the help of heat supplied. In the iron ore sintering process, the heat is supplied majorly by solid fuel. Higher is the solid fuel, more is the formation of Fe<sub>3</sub>O<sub>4</sub> and FeO [2, 3]. The degree of reduction is indicated by the amount of Fe<sub>3</sub>O<sub>4</sub> and FeO. Increase in FeO increases the strength of the sinter. The other mineralogical phase that enhances the strength of the sinter is SFCA. Stronger sinter disintegrates less and renders smooth operation of Blast Furnace. FeO is a crucial parameter that affects the cohesive zone in the Blast Furnace. Fluctuation in FeO leads to undesirable changes in the cohesive zone. In this paper, the effect of waste gas recycling in the Sinter Plant, especially on FeO formation and solid fuel saving, is presented. The reduction of SO<sub>x</sub> and NO<sub>x</sub> emissions is excluded.

Conventionally, the exhaust gas from the Sinter Machine is filtered in ESP and subsequently emitted into the atmosphere. There has been a trend of *recycling sinter waste gas* onto the sinter bed over the last three decades to reduce the usage of solid fossil fuel and emissions [2, 4–12]. Installation of sinter waste gas recycling was primarily aimed at reducing the amount of waste gas through electrostatic precipitator (ESP) in Tobata Sinter Plant No. 3 of Nippon Steel, in 1992 [13]. Sintering waste gas contains CO in the range of 5000–7000 ppm, 6–7% CO<sub>2</sub>, about 150 ppm of SO<sub>x</sub> and 250 ppm NO<sub>x</sub>, 7–8% H<sub>2</sub>O vapor and 14–16% O<sub>2</sub>. The CO concentration is up to

25,000 ppm in certain wind legs. Recycling this waste gas helps in increasing CO concentration in the sinter bed and enhances the formation of magnetite and wüstite. The CO in the recycled waste gas helps in the direct reduction of Fe<sub>2</sub>O<sub>3</sub>, as indicated by Eq. (1), and reduces the solid fuel demand:



Recycling the overall waste gas or a part thereof is called waste gas recycling (WGR). Recycling of waste gas from certain wind boxes containing a higher amount of CO selectively is called selective waste gas recycling (SWGR). Saving of solid fuel in the case of WGR is lower than that in SWGR, as the overall waste gas is lean in CO. By recycling waste gas, the oxygen concentration in the hood is reduced to about 17 to 19%, lowering the combustion efficiency of the solid fuel [14]. The limiting composition of the waste gas is reported as 15% O<sub>2</sub>, 6% CO<sub>2</sub> and 8% H<sub>2</sub>O; deviation in which, may result in the deterioration in the quality parameters of sinter [13].

The other benefit projected by researchers is the reduction in CO<sub>2</sub>, SO<sub>x</sub>, NO<sub>x</sub> emission. It is believed that the dust, SO<sub>x</sub> and NO<sub>x</sub> present in the recycled waste gas are trapped in the sinter bed. The reduction in NO<sub>x</sub> emissions was reported by Chen [4], Han [2], Fan [15] and SO<sub>x</sub> by Ikehara [13]. An increase in productivity with SWGR was reported by Ikehara with an emphasis on controlling the CO, O<sub>2</sub> and H<sub>2</sub>O content in the recycled waste gas. Sintering time increased when O<sub>2</sub> content in the recycled gas was reduced to less than 18% and H<sub>2</sub>O content increased above 10%. Improved mineralogical features coupled with an increment in TI were reported by Iwami [5] when oxygen concentration was increased from 21 to 26%. Injecting oxygen in the sinter bed enhanced the combustion efficiency of solid fuel and the productivity of the Sinter Machine increased [16–18]. To make up the oxygen in WGR, fresh air was blended with waste gas, before entering the recycling hood. As the CO got diluted due to fresh air addition, the benefit in terms of coke saving was compromised.

Iron ore reduction in CO is lowered as the temperature increases [19]. The thickness of the combustion zone is higher in the latter portion of the Sinter Machine and the residence time at high temperature is longer. According to Iwami [16], hematite undergoes thermal dissociation at high temperatures and changes to magnetite. He recommended to increase the residence time at a temperature of 1200–1400 °C to enhance the formation of magnetite, FeO and SFCA. The length of the waste gas recycling hood and its location is critical to the various physicochemical reactions occurring in the combustion zone [6, 7]. At a

higher concentration of oxygen, suppression of reduction reaction was noticed [5, 18]. Hence, injecting waste gas beyond 50% length of the Sinter Machine may not be useful, rather detrimental.

A non-selective waste gas recycling system (WGR) was installed in a Sinter Plant, as shown in Fig. 1. The waste gas emitted into the atmosphere is 1,000,000 m<sup>3</sup>/h, and the volume of recycled waste gas is 300,000 m<sup>3</sup>/h. The hood covers about 70% of the sintering area. An FA Fan supplies atmospheric air into the WGR hood, to make up for the deficiency of oxygen. It was noticed that above 20% of waste gas recycling, the productivity started dropping with a significant decrement in Tumbler Index. Fluctuation in FeO was noticed. The various underlying causes of deterioration in quality parameters were investigated and validated. It was noticed that deficiency of oxygen due to the hood and excessive moisture [13] in the sinter mix contributed largely to the deterioration. These parameters were optimized and a sustainable solution was arrived at.

## 2 Materials and Methods

Pot tests were conducted to find and optimize the parameters affecting FeO formation, the amount of coke replaceability, fines rejection and TI. The pot sinter facility was modified to recycle waste gas recycling, as shown in Fig. 2. The granulated sinter mix was charged into the pot and the top layer was ignited with the help of a burner. After ensuring the top layer was properly ignited, the burner was stopped. The temperature and pressure of the waste gas were measured with the help of transmitters marked as PT and TT respectively, in the image. The maximum static pressure attained in the pot was

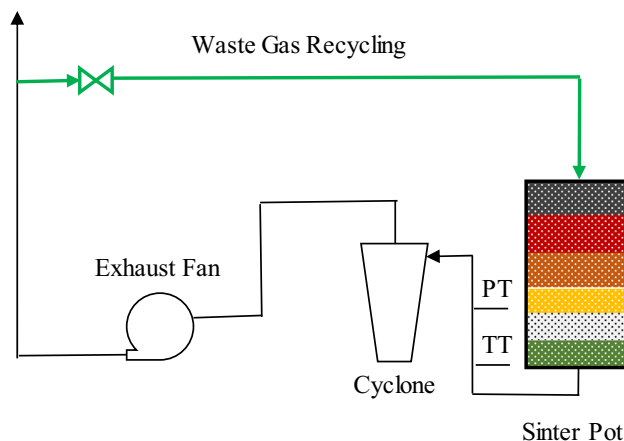


Fig. 2 Pot sinter setup with waste gas recycling

– 50 mBar. The flow of waste gas can be varied with the help of a damper. A thoroughly granulated sinter mix was used to conduct the trials. The chemical composition of the sinter mix and solid fuel used in the pot test is given in Table 1.

A Portable Gas Analyzer PG300 of Horiba make was used to measure the composition of the waste gas. ISO 3271 for Tumbler Index (TI, +6.3 mm) and ISO 4696 for Reduction Degradation Index (RDI, +3.15 mm) respectively were followed to assess the quality of sinter.

Pot test with base case, i.e., without waste gas recycling was conducted first. The process and quality parameters such as suction, waste gas temperature, sinter chemistry, TI and RDI were recorded. Subsequent tests were conducted by increasing the amount of waste gas recycled gradually to 10, 20, 30, 40 and 50%.

Fig. 1 WGR system in the Sinter Plant

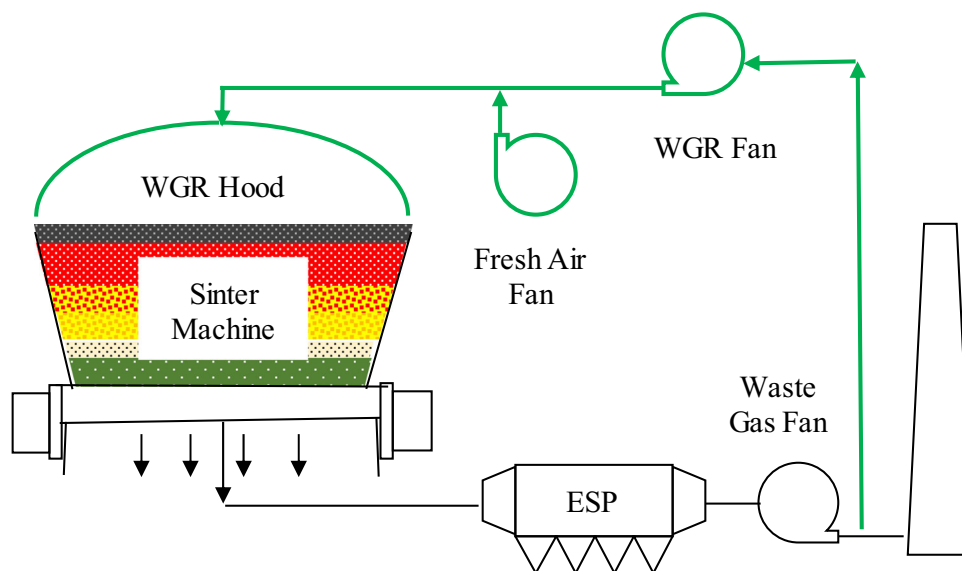


**Table 1** Chemical composition of sinter mix and solid fuel

Sinter mix							Solid fuel		
Fe (%)	SiO <sub>2</sub> (%)	Al <sub>2</sub> O <sub>3</sub> (%)	CaO (%)	MgO (%)	LOI (%)	C (%)	Ash (%)	VM (%)	FC (%)
48.97	4.97	1.91	8.29	1.88	12.39	5.69	9.90	3.54	86.56

### 3 Results and Discussion

The observations during pot tests and operating WGR in the Sinter Plant are presented in this section. Statistical and thermodynamic analysis was carried out and the inferences were used to control the process successfully.

#### 3.1 Pot Tests

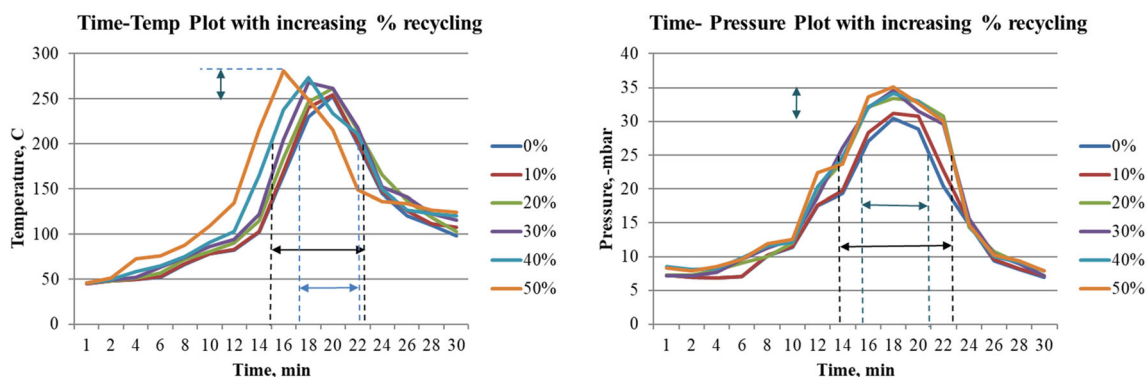
The results of the pot tests are given and discussed below. The waste gas composition measured before recycling was: 15.6% O<sub>2</sub>, 6200 ppm CO, 187 ppm NO<sub>x</sub> and 101 ppm SO<sub>x</sub> and 6.7% CO<sub>2</sub>. The process parameters of pot tests are given in Fig. 3, and the sinter quality parameters are given in Fig. 4. As the recycled waste gas increased, the suction started increasing gradually from – 27 to – 35 mBar and the BTT from 253 to 281 °C. The sintering time decreased from 20 to 16 min, indicating an acceleration in the sintering process. The combustion zone broadening was indicated by the prolonged suction above – 25 mBar and temperature 200 °C in Fig. 3. Reduced sintering time with the increasing amount of waste gas indicated an increase in productivity. Higher suction pressure and prolonged residence time of the combustion zone at higher temperatures is attributed to the enhanced thermal conditions. This condition is favorable for the formation of magnetite, wüstite and SFCA.

As shown in Fig. 4, the FeO in sinter gradually increased from 9 to 11.1% at 40% recycling and dropped to 10.9% at 50% recycling. The increment in FeO at the same coke rate was due to the CO in the waste gas. The more

waste gas was recycled; the more was the FeO formed. An equivalent quantity of coke could be reduced to achieve the target FeO of 9%. The decline beyond 40% of recycling was due to the deficiency of oxygen. The cold strength of sinter indicated as TI, increased from 64 to 65.8% at 40% recycling, beyond which, a decline is evident. – 5 mm sinter rejection increased beyond 30% recycling and kept increasing up to 50%. As an undersize rejection in pot sinter setup, commonly experienced, is in the range of 25%, 30–40% waste gas recycling is considered as a trade-off between the strength advantage and rejection.

#### 3.2 Operational Analysis of WGR

During the erection of the WGR hood segments one by one, the productivity got affected gradually. When WGR was operated at 30% recycling, the speed of the Sinter Machine was decreased by 5%. The parameters of a similar Sinter Machine without WGR, with the same input, were considered for data analysis. An abnormal phenomenon of lower or higher FeO than expected was noticed. A significant drop in TI was noticed, as indicated in Fig. 5. The carbon rate decreased, indicating savings in terms of solid fuel. The impact on RDI was not significant. However, at 20% recycling, the decline in TI and speed was not noticed. As recycling increased to 30%, an adverse impact was experienced. It was also noticed that the performance of the WGR deviated significantly from that in pot tests. Lower productivity, reduced TI at a much lower amount of recycled waste gas was observed. Probable thermodynamic causes of FeO fluctuation such as CO concentration,

**Fig. 3** Time–temperature and time–pressure plots

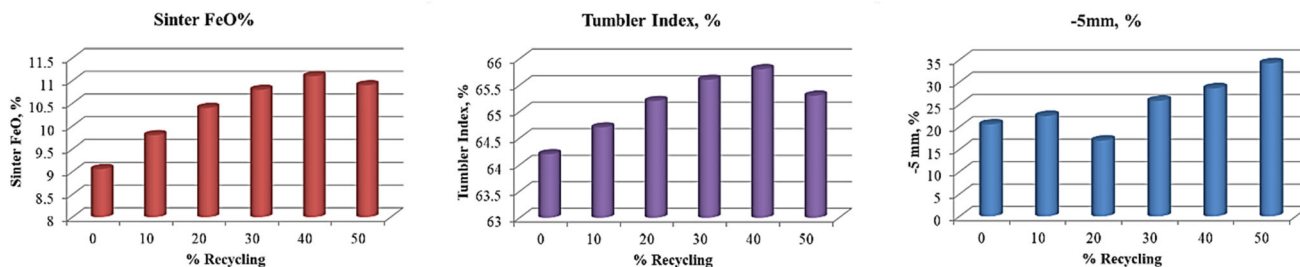


Fig. 4 Sinter FeO, TI and – 5 mm (%) with increasing waste gas recycling

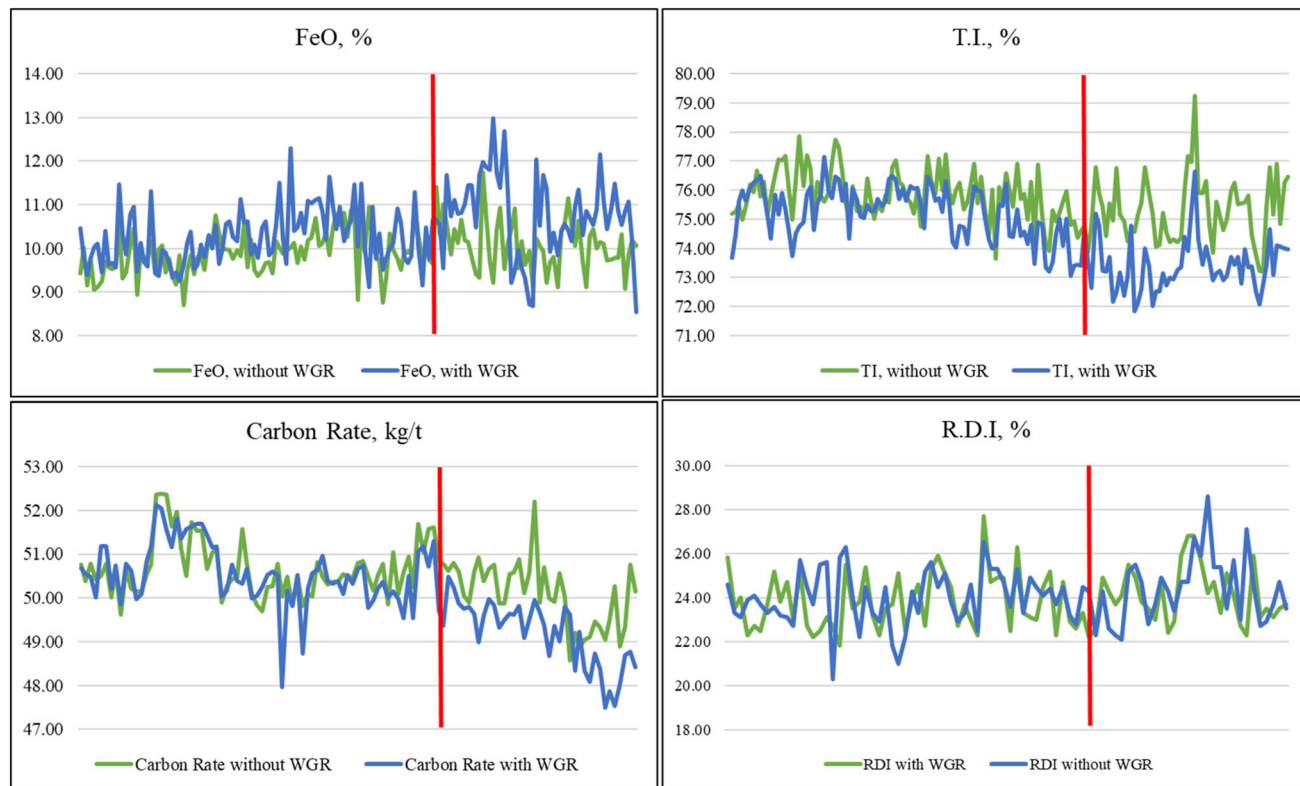


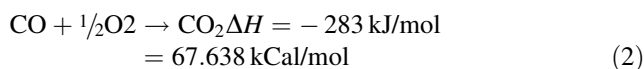
Fig. 5 Comparison of FeO, TI and carbon rate and RDI after starting WGR at 30%

reduction efficiency with CO, the partial pressure of oxygen and unexpected oxidation of magnetite and wüstite if any, were checked and discussed in Sect. 3.3.

The following were the assumptions made in estimating the saving of solid fuel with waste gas recycling:

1. Density of waste gas: 0.6734 kg/m<sup>3</sup> at NTP
2. Calorific value of CO: 2876.23 kcal/m<sup>3</sup>
3. Calorific value of the solid fuel: 7480 kcal/kg
4. Consumption of solid fuel: 58 kg/t of sinter
5. Molarity of CO = 0.045629
6. Sintering temperature 1340 °C

The heat of reaction of CO with oxygen is given in Eq. (2):



The theoretical saving in the solid fuel with varying CO content and the volume of recycled waste gas was calculated, and the typical values are indicated in Table 2.

### 3.3 Rate-Limiting Mechanism

In the iron ore sintering process, the mineralogical phase transformations occur as the process proceeds due to various chemical reactions, solid-state transformations and diffusion. The rate-limiting mechanism in this paper is referred to as the slowest step out of the above lowering the reduction rate. When WGR was operated above 20%

**Table 2** Calculated saving of solid fuel with varying CO content and volume of recycled waste gas

CO content in waste gas (ppm)	2500	3000	3500	4000	4500	5000	5500	6000	6500
Calorific value of waste gas (kCal/m <sup>3</sup> )	7.60	9.12	10.64	12.16	13.68	15.20	16.72	18.24	19.76
Recycled waste gas volume (m <sup>3</sup> /h)	290,000	270,000	250,000	230,000	210,000	190,000	170,000	150,000	130,000
Expected solid fuel saving (kg/t)	1.02	1.22	1.42	1.63	1.83	2.03	2.24	2.44	2.64

recycling, FeO formation was noticed to have a rate-limiting step. Incidental variation in the carbon rate in the sinter mix had led to higher FeO or lower FeO than expected. The difference in carbon rate and FeO during the stabilization and after stabilization of WGR is indicated in Figs. 6 and 7. The data correspond to the two Sinter Machines: with waste gas recycling and without, during the same period with the same inputs. The difference in FeO at low carbon rate and high carbon rate was plotted in ascending order for better visualization. The specification of FeO was 9 to 10 ± 1%. At lower carbon rate, FeO formation receded in the case of WGR to as low as – 2% level. At higher carbon rate, FeO was higher by 3%. The high amount of FeO formed at higher carbon rate was predominant than low FeO formed at lower carbon rate.

The difference in FeO and carbon rate increased after the stabilization of WGR, as shown in Fig. 7. FeO increased by 2.59% at a slightly higher carbon rate of 0.4 kg/t. This essentially indicated the saving of solid fuel with WGR. FeO decreased by 1.7% when the carbon rate dropped by 0.67 kg/t. When carbon rate increased by 1.23 kg/t, FeO increased by 2.12%. At much higher drop in the carbon rate of 2.68 kg/t, FeO decreased by 0.63% only. The nonlinear behavior was analyzed by logarithmic and exponential plots as shown in Fig. 8. Analyzing the normalized data in quadrant 2 in Fig. 6 (negative dCr and positive dFeO), the following empirical relation was derived:

$$d\text{FeO} = 1.3d\text{Cr} + 2.4378 \quad (3)$$

Ideally, FeO formation is expected to follow the above trend when the CO utilization is maximum. But the

difference in FeO followed a logarithmic trend with a good  $R^2$  value, as shown in Fig. 8b.

The following correlation was derived from Fig. 8:

$$y = 0.9422 \ln(x) - 2.4726 \text{ or } y = 0.9377e^{0.0762x} \quad (4)$$

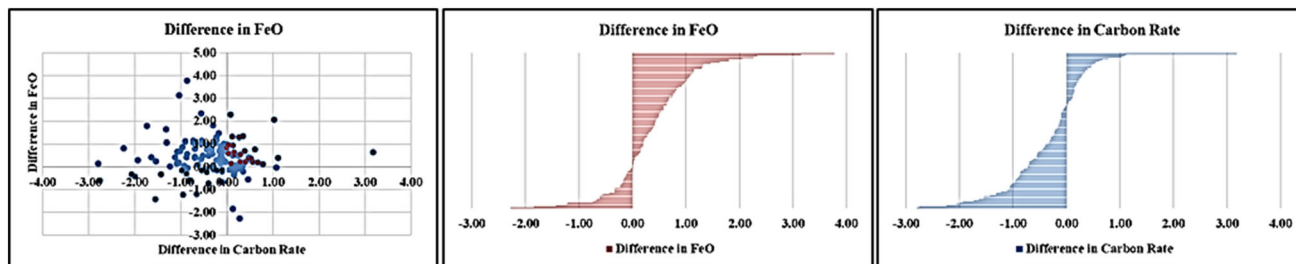
According to the above statistical analysis, to limit the fluctuation in FeO to ± 1%, the variation in the carbon rate should be restricted within 0.28 to 1.26 kg/t or  $0.77 \pm 0.49$  kg/t. The accuracy of the prediction was calculated as 99.12%. The deviation from the prediction could be attributed to the abnormal thermodynamic conditions.

Thermodynamically, the formation of FeO depends on the partial pressure of oxygen and CO. With waste gas recycling, the CO generated due to the combustion of solid fuel comes back to the sinter bed and enriches the waste gas giving more opportunity for direct reduction of iron ore particles. The feasibility of the reduction of Fe<sub>2</sub>O<sub>3</sub> with CO, oxidation of Fe<sub>3</sub>O<sub>4</sub> and FeO with O<sub>2</sub> has been verified as illustrated below. The standard thermodynamic data [20, 21], as given in Table 3, were used to verify the reactions in sintering conditions. The temperature of the combustion zone was considered as 1340 °C (1613 K), and the  $\Delta G_T$  of four reactions is given in Table 4.

The hematite got reduced to magnetite by the CO which was produced due to the combustion of coke and increasing temperature. As shown in Table 1(b), the reaction was spontaneous (negative  $\Delta G_T$ ). The partial pressure could be verified as shown below:



Equilibrium constant  $K = (a^2 \text{Fe}_3\text{O}_4 \cdot a \text{CO}_2)/(a^3 \text{Fe}_2\text{O}_3 \cdot a \text{CO})$  [20]

**Fig. 6** Difference in FeO and carbon rate during WGR stabilization

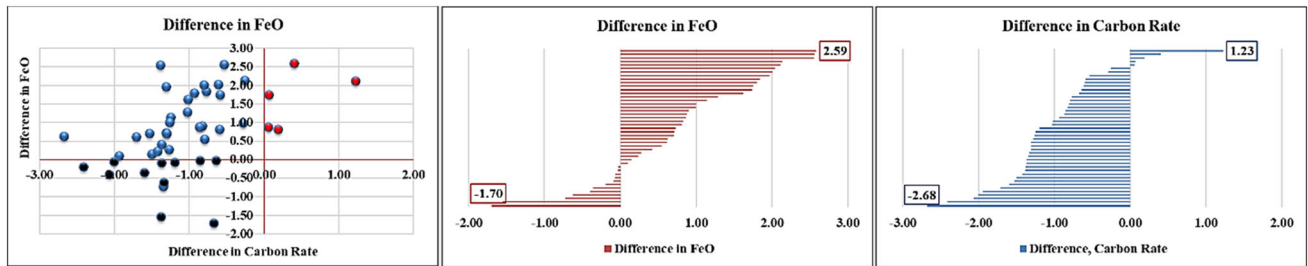


Fig. 7 Difference in FeO and carbon rate after WGR stabilization

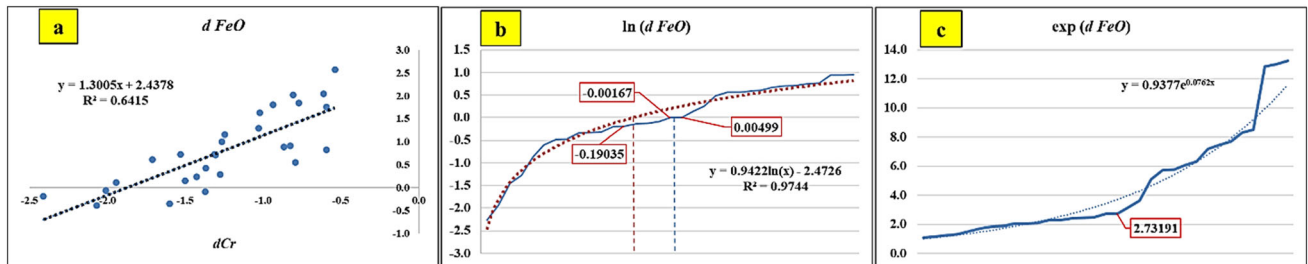


Fig. 8 a Difference in FeO in quadrant 2, b natural log of difference in FeO, c exp of difference in FeO

Table 3 Standard thermodynamic data [21]

Species	Enthalpy (kJ/mol)	Entropy (J/K/mol)	Gibbs free energy (kJ/mol)
Fe <sub>2</sub> O <sub>3</sub> (s)	− 824.248	87.40376	− 742.2416
Fe <sub>3</sub> O <sub>4</sub> (s)	− 1118.38	146.44	− 1015.4568
FeO (s)	− 271.96	60.75168	− 251.4584
CO (g)	− 110.541	197.9032	− 137.27704
CO <sub>2</sub> (g)	− 393.505	213.6769	− 394.38384
O <sub>2</sub> (g)	0	205.0286	0

Table 4 Gibbs free energy change of the reactions

Reaction	$\Delta H$ (kJ/mol)	$\Delta S$ (J/K/mol)	Standard $\Delta G$ (kJ/mol)	$\Delta G_T = \Delta H - T\Delta S$
3 Fe <sub>2</sub> O <sub>3</sub> + CO = 2 Fe <sub>3</sub> O <sub>4</sub> + CO <sub>2</sub>	− 46.9863	46.4424	− 61.2956	− 115.3959752
4 Fe <sub>3</sub> O <sub>4</sub> + O <sub>2</sub> = 6 Fe <sub>2</sub> O <sub>3</sub>	− 471.955	− 266.366	− 391.6224	− 79.59809378
Fe <sub>3</sub> O <sub>4</sub> + CO = 3 FeO + CO <sub>2</sub>	19.53928	51.58872	3.9748	− 56.45090456
4 FeO + O <sub>2</sub> = 2 Fe <sub>2</sub> O <sub>3</sub>	− 560.656	− 273.228	− 478.6496	− 158.1915213

Considering activity of Fe<sub>2</sub>O<sub>3</sub> and Fe<sub>3</sub>O<sub>4</sub> as unity and  $p_{CO} + p_{CO_2} = 1$ ,

$$p_{CO_2}/p_{CO} = 1.055826$$

$$p_{CO} = 0.48642.$$

In other words, CO content should be more than 4864.2 ppm minimum, for the above reaction to occur. At low CO in WGR and low carbon rate, the above

condition was not fulfilled and therefore the FeO formed was lower than expected.

The composition of recycled waste gas by varying the speed of WGR Fan and FA Fan is shown in Table 5. The H<sub>2</sub>O content was considered as 5.5%. The composition of the exhaust gas with and without WGR is given in Table 6. It was observed that about 250 ppm of CO and 1.1% of CO<sub>2</sub> got reduced in the exhaust gas due to WGR. The

**Table 5** Composition of the recycling waste gas and number of moles of carbon, oxygen and nitrogen

CO (ppm)	CO (%)	CO <sub>2</sub> (%)	O <sub>2</sub> (%)	N <sub>2</sub> (%)	nC	nO	nN
1390	0.1390	2.14	19.80	72.42	0.022790	0.495190	1.448420
2877	0.2877	4.16	18.19	71.86	0.044477	0.504877	1.437246
3129	0.3129	4.35	18.00	71.84	0.046629	0.505129	1.436742
2413	0.2413	3.06	19.80	71.40	0.033013	0.514613	1.427974
1609	0.1609	2.46	21.50	70.38	0.026209	0.535809	1.407582
2380	0.2380	3.33	19.63	71.30	0.035680	0.516580	1.426040
2423	0.2423	3.59	19.88	70.79	0.038323	0.526823	1.415754
2499	0.2499	3.75	19.78	70.72	0.039999	0.528099	1.414402
2600	0.2600	3.90	19.80	70.54	0.041600	0.531600	1.410800
2800	0.2800	4.34	19.73	70.15	0.046200	0.539200	1.403000
1890	0.1890	2.52	21.76	70.03	0.027090	0.542490	1.400620

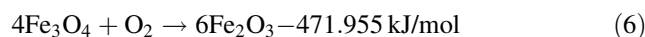
**Table 6** Composition of the exhaust gas

	CO (ppm)	CO <sub>2</sub> (%)	O <sub>2</sub> (%)	NO <sub>x</sub> (ppm)
WGR not running	6041	8.06	13.79	238
	6010	8.05	13.75	238
WGR running	5746	9.18	12.49	206
	5773	9.14	13.41	199

variation of the waste gas composition with increasing FA Fan speed is provided in Fig. 9.

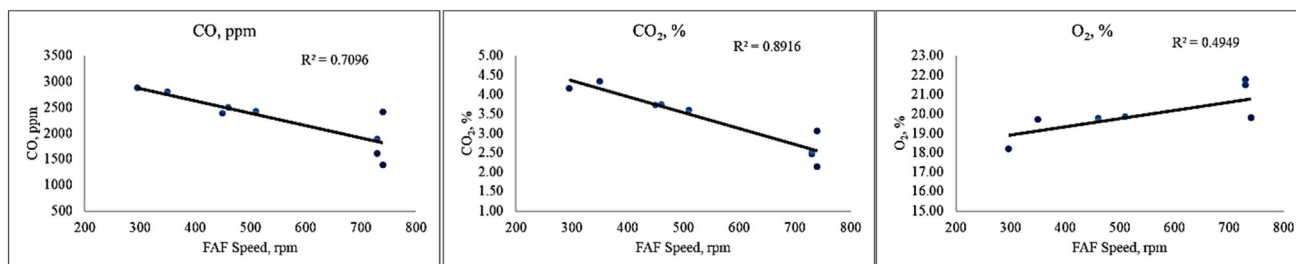
The flow and composition of recycled waste gas were adjusted with the aid of FA Fan speed.

The partial pressure of oxygen is an important parameter that influences the formation of various mineralogical phases in the sinter. Researchers [16–18, 22–27] have established desired oxygen partial pressure to achieve optimum SFCA phase in iron ore sinter. The viscosity of the melt and its composition is greatly influenced by oxygen partial pressure. The stability of magnetite is maximum at  $10^{-5}$  to  $10^{-6}$  atm oxygen partial pressure. Reduction of iron oxide at high temperature in CO and related kinetic aspects were investigated [28]:



At maximum sintering temperature, i.e., 1340 °C, free energy change for the above reaction was  $\Delta G_T = -41.84$  kJ/mol and the partial pressure of oxygen was  $10^{-5}$ . The temperature dependency of  $-\Delta G_T$  of oxidation reactions is shown in Fig. 10, indicating that free energy change increased with temperature. Hence to avoid oxidation of magnetite and FeO, high temperature should be avoided, i.e., the WGR hood need not be extended beyond 50% of the Sinter Machine length.

With the oxygen content in waste gas in the range of 18–19.8%, the partial pressure of oxygen is  $4.9\text{--}5.4 \times 10^{-4}$  atm and the stability of magnetite may be affected. Hence, it can be deduced that 15% oxygen in the

**Fig. 9** Variation of waste gas composition with FA Fan speed



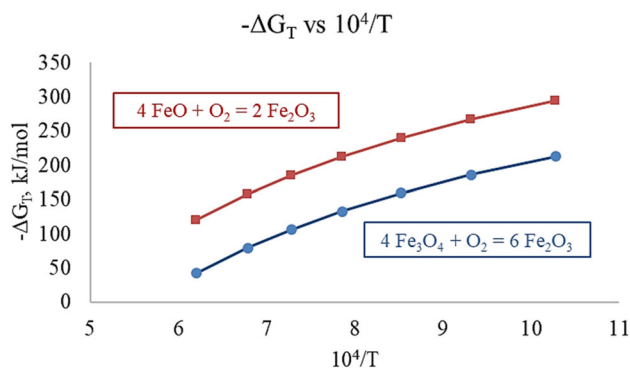
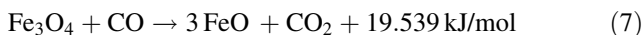


**Fig. 10** Temperature dependency of  $-\Delta G_T$

waste gas is the limiting value, above which the above reaction is feasible, meaning oxidation of magnetite to hematite is possible. Hence, additional care should be taken to suppress the above reaction.

FeO (Wüstite) was another important phase that influenced the cold strength of the iron ore sinter, apart from SFCA. Its formation from magnetite with CO was an endothermic reaction. It had positive entropy and negative  $\Delta G_T$ , as shown in Table 1b, and was spontaneous. Similarly, the oxidation of FeO was also spontaneous and hence reducing conditions were needed to achieve maximum benefit:



The  $\Delta H$  in Eqs. 5 and 7 is much higher than the rest. Therefore, it is inferred that the oxidation of FeO and  $\text{Fe}_3\text{O}_4$  needs to be taken care. The order of solid-state reactions with increasing temperature [16, 18, 28] is given below:

1. 800 °C: FeO formation started
2. 900 °C: Reduction of  $\text{Fe}_3\text{O}_4$  to FeO ended
3. 1000 °C: Reduction of  $\text{Fe}_2\text{O}_3$  to  $\text{Fe}_3\text{O}_4$

As seen from the above, the reduction of  $\text{Fe}_2\text{O}_3$  to  $\text{Fe}_3\text{O}_4$  with CO is much easier than  $\text{Fe}_3\text{O}_4$  to FeO (owing to the significant difference in the heat of reaction). Unless sufficient heat is provided through solid fuel, the formation of FeO with CO will be affected. Hence, low FeO was experienced than expected at lower carbon rate. The designed hood pressure of 0.3 mBar (0.000296 atm) is another key parameter that influences the rate of reduction with CO. When corrected to 1 atm, the actual CO content in the recycled gas after blending with fresh air was measured as 2200–3100 ppm; which is too low.

During the reduction of porous iron ore particles with CO gas, the gas diffuses through the pores, followed by oxygen removal via phase boundary [19], to join back the stream of gas. High-temperature diffusion remains

unaffected as seen in the case of hard iron ore particles with very low porosity. Here the reduction with gas becomes the rate-limiting step. To achieve the same amount of FeO, the hard iron ore particle needs more heat, through solid fuel. Meaning porous particles are deriving benefit from waste gas recycling than hard particles. In the real situation, we have a wide range of particles with varying hardness, porosity and angularity; deviating from theoretical conditions. Hence, we see a wide variation of FeO and SFCA formation among particles. In the sintering process, the bulk flow through voidage between particles is many folds greater than the effusion through pores and micropores within the particles; until the combustion zone is reached. Due to the presence of liquid in the combustion zone, greater resistance is offered to the gas flow [29] and the effusion through micropores increases.

In the case of high carbon rate, the thickness of the combustion zone and the residence time at elevated temperature is high [30]; allowing higher utilization of CO. On the contrary, the thin combustion zone in the case of low carbon rate does not offer much resistance to the flow of waste gas and the CO utilization rate is poor resulting in lower FeO than expected.

The variation of FeO and moisture is given in Fig. 11. The moisture variation has been restricted to  $7.8 \pm 0.6\%$ . The boundary limits derived from the statistical analysis and rate-limiting mechanism, namely carbon rate  $0.77 \pm 0.5 \text{ kg/t}$  and oxygen  $> 19\%$ , have been maintained to achieve consistent performance. The countermeasures taken are given below:

1. Optimization of the fresh air fan speed.
2. Additional windows in the hood were provided to ensure sufficient fresh air supply when the WGR is not operational.
3. Sinter mix moisture was controlled in the range of  $7.8 \pm 0.6\%$  by installing an additional moisture gauge just before charging the sinter mix into the Sinter Machine. The standard deviation in the moisture was reduced from 0.5 to 0.186.

## 4 Conclusions

The following conclusions are drawn:

1. The deterioration in quality parameters beyond 40% recycling is evidenced in the pot tests.
2. High carbon rate results in greater residence time at elevated temperature and higher utilization of CO through waste gas.
3. Poor CO utilization is experienced at low carbon rate due to low resistance of the combustion zone and

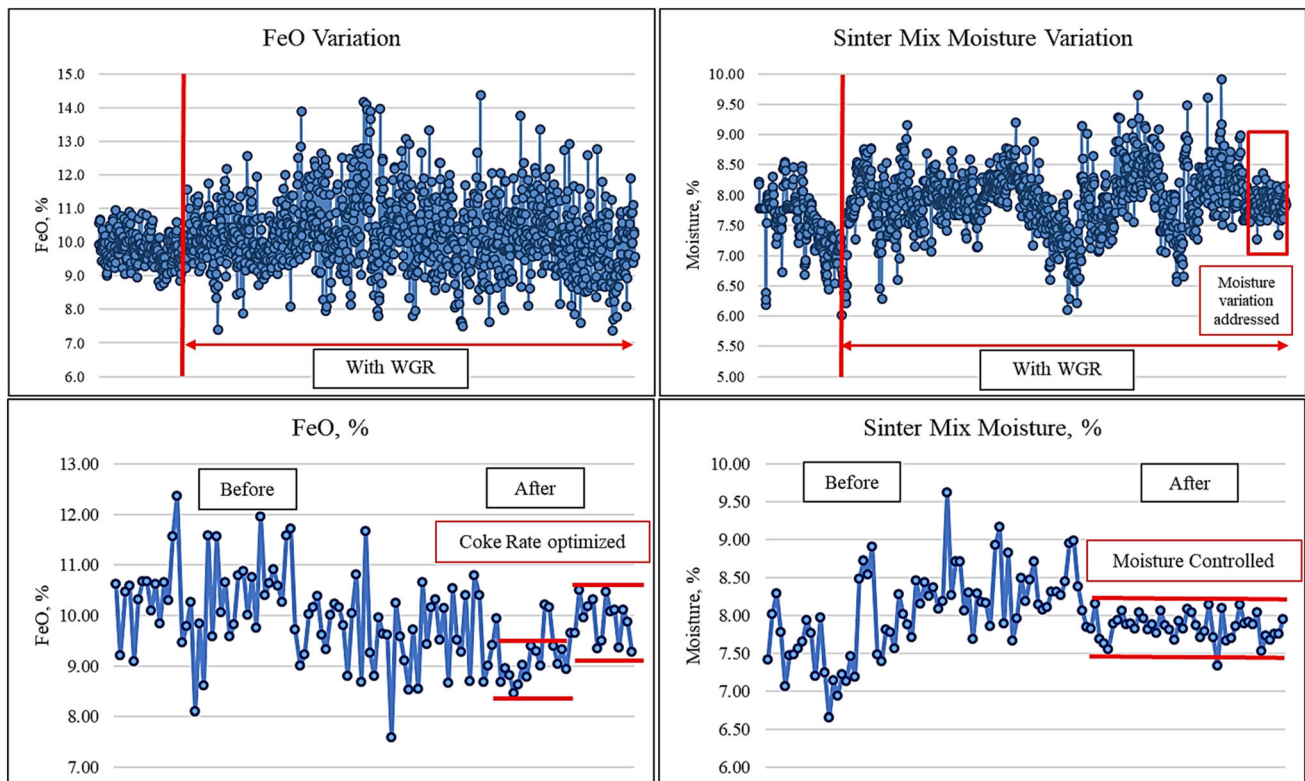


**Fig. 11** Variation of FeO and sinter mix moisture controlled

higher heat demand of FeO formation from  $\text{Fe}_3\text{O}_4$  with CO.

4. The combustion efficiency of solid fuel is affected due to low oxygen availability in the WGR hood.
5. The thermodynamic analysis suggests that the minimum CO content required is 4864 ppm, and the variation in carbon rate should be less than  $\pm 0.5$  kg/t.
6. The formation of FeO from hematite and magnetite with CO (Eqs. 1 and 6) is affected due to the rate-limiting mechanism at 1200 °C and above.
7. Oxidation of  $\text{Fe}_3\text{O}_4$  and FeO (Eqs. 5 and 7) is also possible at high temperatures, low CO and high  $\text{O}_2$  content in the recycled gas. Hence, injection of waste gas in the latter part of the Sinter Machine may be avoided.

**Acknowledgments** The authors express their gratitude to the Sinter Plant collective for their support in installing a waste gas recycling system in the pot sinter facility, during the pot tests and optimization of WGR.

**Conflict of interest** The authors declare that there is no conflict of interest.

## References

- [1] Loo C, *ISIJ Int* **45** (2005) 436. <https://doi.org/10.2355/isijinternational.45.436>.
- [2] Han J, Lou G, Zhang S, Wen Z, Liu X, Liu J, *Energies* **12** (2019) 1 <https://doi.org/10.3390/en12203828>.
- [3] Cores A, Verdeja LF, Ferreira S, Mochon J, *DYNA* **80** (2013) 152.
- [4] Chen YG, Guo ZC, Wang Z, *ISIJ Int* **48** (2008) 1517. <https://doi.org/10.2355/isijinternational.48.1517>.
- [5] Iwami Y, Yamamoto T, Higuchi T, Oyama N, Sato M, Sodani Y, *ISIJ Int* **55** (2015) 2350. <https://doi.org/10.2355/isijinternational.ISIJINT-2015-322>.
- [6] Zhang S, Wen Z, Wang G, Dou R, Liu X, Li X, *Ironmak Steelmak* **47** (2020) 368. <https://doi.org/10.1080/03019233.2018.1521565>.
- [7] Vanderheyden B, Van Loo F, Mathy C, Pierret JC, *AISTech Iron Steel Technol Conf Proc* **1** (2015) 563.
- [8] Jeong EH, Park JI, Cho BK, *Proc World Congr Mech Chem Mater Eng* **54** (2017) 11159. <https://doi.org/10.11159/mmm17.132>.
- [9] Zhang XH, Feng P, Xu JR, Feng P, Xu JR, Feng LB, Qing S, *Energy* **192** (2020) 116660. <https://doi.org/10.1016/j.energy.2019.116660>.
- [10] Cheng Z, Wang J, Wei S, Guo Z, Yang J, Wang Q, *Appl Energy* (2017). <https://doi.org/10.1016/j.apenergy.2017.06.024>.
- [11] Gan M, Fan XH, Yu ZY, Chen XL, Ji Z, Lv W, Liu S, Huang YS, *Ironmak Steelmak* (2016). <https://doi.org/10.1080/03019233.2015.1136114>.
- [12] Cores A, Verdeja LF, Ferreira S, Ruiz-Bustanza S, Mochón J, Robla JI, González Gasca C, *Dyna* **82** (2015) 227. <https://doi.org/10.15446/dyna.v82n190.44054>.

- [13] Ikehara S, Kubo S, Terada Y, Sakuragi J (1996) Application of exhaust gas recirculation system at Tobata No. 3 sinter plant. Nippon Steel Tech. Rep. 55.
- [14] Fan X, Yu Z, Gan M, Yu Z, Gan M, Jiang T, Wen H, *ISIJ Int* **54** (2014) 2541. <https://doi.org/10.2355/isijinternational.54.2541>.
- [15] Fan X, Yu Z, Gan M, Chen X, Chen Q, Liu S, Huang Y, *ISIJ Int.* (2015). <https://doi.org/10.2355/isijinternational.ISIJINT-2015-180>.
- [16] Oyama N, Iwami Y, Yamamoto T, Machida S, Higuchi T, Sato H, Nishioka K, *ISIJ Int* **51** (2011) 913. <https://doi.org/10.2355/isijinternational.51.913>.
- [17] Jeon JW, Jung SM, Sasaki Y, *ISIJ Int* **50** (2010) 1064. <https://doi.org/10.2355/isijinternational.50.1064>.
- [18] Iwami Y, Yamamoto T, Higuchi T, Nushiro K, Sato M, Oyama N, *ISIJ Int* **53** (2013) 1633. <https://doi.org/10.2355/isijinternational.53.1633>.
- [19] Spreitzer D, Schenk J, *Steel Res Int* **90** (2019). <https://doi.org/10.1002/srin.201900108>.
- [20] Darken LS, Darken LS, Gurry RW, Bever MB, *Physical Chemistry of Metals*, McGraw-Hill, New York (1953).
- [21] Dean JA, *Lange's Handbook of Chemistry*, 15th edn, McGraw-Hill, London (1999).
- [22] Webster NAS, Pownceby MI, Pattel R, Manuel JR, Kimpton JA, *ISIJ Int* **59** (2019) 263. <https://doi.org/10.2355/isijinternational.ISIJINT-2018-573>.
- [23] Chen C, Lu L, Jiao K, *Minerals* **9** (2019) 361. <https://doi.org/10.3390/min9060361>.
- [24] Scarlett NVY, Pownceby MI, Madsen IC, Christensen AN, *Metall Mater Trans B Process Metall Mater Process Sci* **35** (2004) 929. <https://doi.org/10.1007/s11663-004-0087-4>.
- [25] Wang Z, Pinson D, Chew S, Pinson D, Chew S, Monaghan BJ, Pownceby MI, Webster NAS, *ISIJ Int* **56** (2016) 1138. <https://doi.org/10.2355/isijinternational.ISIJINT-2015-598>.
- [26] Webster NAS, Pownceby MI, Madsen IC, Kimpton JA, *ISIJ Int* **53** (2013) 774. <https://doi.org/10.2355/isijinternational.53.774>.
- [27] Webster NAS, Pownceby MI, Madsen IC, Kimpton JA, *Metall Mater Trans B* **43** (2012) 1344. <https://doi.org/10.1007/s11663-012-9740-5>.
- [28] Chen Z, Zeilstra C, van der Stel J, Sietsma J, Yang Y, *Ironmak Steelmak* (2019). <https://doi.org/10.1080/03019233.2019.1589755>.
- [29] Zhou H, Zhou M, Liu Z, Cheng M, Qiu M, Cen K, *ISIJ Int* **55** (2015) 2556. <https://doi.org/10.2355/isijinternational.ISIJINT-2015-311>.
- [30] Ohno KI, Noda K, Nishioka K, Noda K, Nishioka K, Maeda T, Shimizu M, *J Iron Steel Inst Jpn* **101** (2015) 184. <https://doi.org/10.2355/tetsutohagane.101.184>.

**Publisher's Note** Springer Nature remains neutral with regard to jurisdictional claims in published maps and institutional affiliations.